Applied Geochemistry xxx (xxxx) xxx

Contents lists available at ScienceDirect

Applied Geochemistry

journal homepage: http://www.elsevier.com/locate/apgeochem

Boron speciation and extractability in temperate and tropical soils: A multi-surface modeling approach

Elise Van Eynde *, Liping Weng, Rob N.J. Comans

Soil Chemistry and Chemical Soil Quality Group, Wageningen University, 6708, PB, Wageningen, the Netherlands

ARTICLE INFO

Editorial handling by Prof. M. Kersten

Keywords:
Boron
Geochemical multi-surface model
HNO_3
Mannitol
KH_2PO_4
Humic acids
Ferrihydrite

ABSTRACT

Boron is an essential micronutrient for plants, but can also be toxic when present in excess in the soil solution. A multi-surface geochemical model was used to assess the important processes that affect the distribution of the geochemically reactive B in soils over the solution and solid phase. The multi-surface model was based on the adsorption of B on dissolved and solid humic acids, representing reactive organic matter, ferrihydrite, representing the Fe and Al (hydr)oxides, and clay mineral edges. In addition, the performance of previously proposed extraction methods for measuring reactive B was evaluated. Based on B measured in 0.01 M $CaCl_2$ soil extracts (7–85 μmol kg^{-1} soil), we calculated the reactive boron concentration for 5 temperate and 5 tropical soils (8–106 μmol kg^{-1} soil). We found that extractions with 0.43 M HNO_3 or with 0.2 M mannitol + 0.1 M triethanolamine buffer extract on average 240 and 177% of the reactive B predicted by the model, thus releasing additional B that is assumed to be not or only very slowly available for exchange with the soil solution. Reactive B calculated by the model corresponded best to the B measured in a 0.05 M KH_2PO_4 (pH 4.5) extraction. In general, the multi-surface modeling showed that 68% or more of reactive boron was present in the solution phase for the soils in this study and that the adsorption was dominated by oxides in the tropical soils, while solid organic matter was the main adsorbent in the temperate soils. When changing the soil pH($CaCl_2$), B concentration was found to decrease with increasing pH, and both experimental data and modelling suggests that this effect is mainly due to increased binding of B to organic matter.

1. Introduction

Boron (B) is an essential micronutrient for plant growth and development (Uluisik et al., 2018). Boron deficiencies are widespread around the globe, often in weathered acidic soils or calcareous soils with high pH (Shorrocks, 1997). On the other hand, B can also be toxic when present in excess in the soil solution (Gupta et al., 1985; Howe, 1998). Therefore, B requires accurate nutrient management, which demands a thorough understanding of B speciation in soils and the processes that control B bioavailability.

Total B content in soils can go up to 8000 μmol kg^{-1} (Kabata-Pendias and Pendias, 2001), of which a large part is present in primary minerals, or occluded in secondary minerals (Hou et al., 1994). There are also studies showing that most of the total B in soils is part of the organic matter fractions (Kot et al., 2012). These total pools of B are not directly available for plants, as there is no relation between B uptake by plants and total B in soils (Chaudhary and Shukla, 2003; Jin et al., 1987). Plants take up B from the soil solution as boric acid ($B(OH)_3$) (Dordas et al., 2000) and B concentrations in soil solutions often range between 1 and 300 μmol L^{-1} (Kabata-Pendias and Pendias, 2001). The B that originates from mineralization of fresh organic matter, weathering of minerals or atmospheric deposition (Park and Schlesinger, 2002) enters the reactive B pool and is distributed over the solid and solution phase by adsorption/desorption processes. Despite the fact that B is relatively mobile compared to the other micronutrients (Kabata-Pendias and Pendias, 2001), it has been stated by various authors that the adsorption onto reactive soil surfaces controls the B in solution, and therefore regulates B bioavailability, potential toxicity and leaching (Goldberg, 1997; Keren et al., 1985). Adsorption studies of B have focused on organic matter (Goldberg, 2014a; Gu and Lowe, 1990; Keren and Communar, 2009; Lemarchand et al., 2005), clay minerals (Goldberg, 1999; Goldberg and Glaubig, 1986b; Keren and Mezuman, 1981; Manning and Goldberg, 1996; Sims and Bingham, 1967), poorly crystalline Al and Fe oxides (Goldberg, 1999; Peak et al., 2003; Su and Suarez, 1995; Van Eynde et al., 2020) and crystalline oxides (Goldberg, 1999; Goli et al., 2011). In general, it has been found that B adsorption

* Corresponding author.
E-mail address: elise.vaneynde@wur.nl (E. Van Eynde).

https://doi.org/10.1016/j.apgeochem.2020.104797
Received 19 June 2020; Received in revised form 24 September 2020; Accepted 22 October 2020
Available online 31 October 2020

on these mineral and organic reactive surfaces increases with increasing pH, and that the maximum adsorption occurs at pH between 8 and 10, after which the adsorption decreases again. A similar pH-dependent adsorption behavior has been found for B adsorption in soils (Goldberg, 2004; Goldberg et al, 1993, 1996; Goldberg and Glaubig, 1986a). Van Eynde et al. (2020) have shown with a multi-surface modeling simulation that pH can also determine the relative importance of each of these reactive surfaces for B adsorption: in the acidic region, oxides may be more important whereas organic matter may bind most of the B in the alkaline region. However, these modeling simulations have not yet been validated for soil samples.

Geochemical surface complexation models (SCM) are powerful tools to enhance the quantitative understanding of the speciation of trace elements in the soil environment, and processes that affect their bioavailability. The constant capacitance model (CC) has been used mostly to model B adsorption behavior in soils (Goldberg, 1999, 2004). Goldberg et al. (2004; 2000; 2005) have used the CC model to describe pH-dependent B adsorption in soil systems, considering the soil as one type of plane for surface reactions in a generalized composite approach (Goldberg, 2014b). Binding constants were fitted to pH dependent B adsorption data for the soil-specific assemblage (Goldberg et al., 2004), and as a result are not generically applicable to other soils. To make the constants more widely usable, Goldberg et al. (2000) used regression models to relate these binding constants for B adsorption in soils to the surface area, organic carbon, inorganic carbon and Al content, which suggests that different surfaces are playing a role in B adsorption among soil types. The use of the CC model for modeling ion speciation in soils does not take into account the specific characteristics (i.e., binding capacities, affinities, heterogeneity of surface sites) of each of the reactive surfaces, which makes it difficult to assign relative importance to the different reactive surfaces for B adsorption. Conversely, a multi-surface or assemblage modeling approach combines separate models for ion binding to the different reactive surfaces (Groenenberg and Lofts, 2014; Weng et al., 2001). Examples of such models that have been recently parameterized for B are the Charge Distribution and Multi Site Complexation model (CD-MUSIC) for modeling adsorption on oxides (Goli et al., 2011; Van Eynde et al., 2020), or the Non-ideal Competitive Adsorption (NICA) Donnan model for modeling adsorption on organic matter (Goli et al., 2019).

No attempts have yet been made to model the speciation of naturally occurring B in soils instead of modeling adsorption experiments with added B (Goldberg, 1999, 2004). Modeling the partitioning of natural B over the solid and solution phase requires an estimation of the geochemically reactive concentration of B in soils. The reactive concentration is considered as potentially available for uptake by plants, and is the concentration that is distributed over the solid and solution phase through adsorption/desorption and precipitation/dissolution equilibria (Groenenberg et al., 2017). The actual available pool in solution then depends on the reactive concentration, pH, content of reactive surfaces and competing ions, and is often approximated by extraction with weak salts (Degryse et al., 2009) such as $CaCl_2$ (Houba et al., 2000). Recently, an ISO standard has been developed to extract the geochemical reactive pool of trace elements, using a dilute nitric acid solution at approximately pH 0.5 (ISO, 2016). The method has been evaluated for a wide range of trace elements based on geochemical multi-surface modeling, but not for B (Groenenberg et al., 2017). Others have used alternative extraction solutions as part of fractionation schemes to quantify the adsorbed B, such as KH_2PO_4 (Hou et al, 1994, 1995) that is based on ligand exchange between B and phosphate (PO_4) on reactive surfaces, or polyols that are known to form soluble complexes with B (Bingham, 1982; Goldberg and Suarez, 2014; Jin et al., 1987).

In this study, we will use a multi-surface modeling approach for simulating natural B speciation in both temperate and tropical soil samples. Boron speciation and extractability may differ between these two climatic regions due to differences in content of important reactive soil surfaces and mineralogy. The first aim is to evaluate the use of different previously proposed extraction methods (0.05 M KH_2PO_4, 0.2 M mannitol (pH 7.3) and 0.43 M HNO_3), based on different B-exchange principles, for estimating the reactive B. The calculated reactive B with a multisurface model will be compared with the B measured in the three different extraction methods. Secondly, we aim to evaluate which soil surfaces control B speciation in temperate and tropical soils in relation to soil properties and pH.

2. Material and methods

2.1. Soil analyses

Two sets of air dried top soil samples were used for extractions and modeling of the soil B. The first set consisted of 5 temperate top soil samples from the Netherlands. These are samples taken from sandy, clay or clay-peat arable fields. The second set consisted of 5 tropical top soil samples from arable fields in Burundi. These 5 samples were selected out of a larger set of soil samples (n = 15) that were taken from different locations in the country. All 5 soils are classified as Ferralsol based on their geo-referenced location (Hengl et al., 2017).

The solution concentration of B (B–$CaCl_2$), dissolved organic carbon (DOC) and pH($CaCl_2$) were measured in extracts of 0.01 M $CaCl_2$ (Houba et al., 2000). Calcium chloride extractions have often been used as a proxy for the soil solution, and to validate multi-surface models that aim to model the solid-solution partitioning of ions (Degryse et al., 2003; Dijkstra et al., 2009; Groenenberg et al., 2017; Weng et al., 2001). A 0.01 M $CaCl_2$ was freshly prepared in a plastic volumetric flask, in order to avoid B contamination from glassware. A fixed volume of this solution was added to the soil samples at a solution-to-solid ratio (SSR) of 10 in polypropylene centrifuge tubes. The suspensions were equilibrated in a horizontal shaker at 180 oscillations $minute^{-1}$ for 24 h and were afterwards centrifuged for 10 min at 1800 *g* and filtered over a 0.45 μm membrane filter. The B–$CaCl_2$ was measured in an acidified subsample of the supernatant, using High Resolution Inductively Coupled Plasma Mass Spectrometry (HR-ICP-MS, Element 2, Thermo Scientific) with a Teflon nebulizer and spray chamber instead of (boron-silicate) glass. All measurements were done in duplicate and average values were used as final estimates for B–$CaCl_2$ concentrations. The average difference between both B measurements was around 10% of the average concentration. The average B concentrations of the blanks (n = 5) was 0.4 ± 1.1 μg L^{-1}.

The pH($CaCl_2$) was measured using a glass electrode, from which no significant B release was found (results not shown). The dissolved total carbon and dissolved inorganic carbon concentrations were measured in a non-acidified supernatant with an Segmented Flow Analyzer (SFA-TOC, San++, Skalar) equipped with an IR detector that measures the amount of $CO_{2(g)}$ after an internal acidification and destruction step, and the DOC concentrations were calculated as the difference between total and inorganic carbon. The inorganic phosphate (PO_4–$CaCl_2$) concentration in the $CaCl_2$ extraction was measured by the molybdenum-blue method (Murphy and Riley, 1962) using a fully automated segmented flow analyzer (SFA-PO_4).

The clay content in the Burundi soils was measured by laser-diffraction analysis (Konert and Vandenberghe, 1997). Soils (0.5–1.5 g) were pre-treated three times with H_2O_2 and once with HCl, while standing in a warm water bath. Before analysis, the pre-treated samples were suspended in water (~200 ml) which was removed and replaced with fresh ultra-pure water for multiple times to remove excess of salts. The measured volume percentage of the fraction smaller than 2 μm was re-calculated to the mass percentage of clay using a particle density of 2.6 g cm^{-3} and a bulk density of 1.3 g cm^{-3}. The clay content from the Dutch soils was derived by the accredited laboratory of Eurofins Agro Netherlands via Near-Infrared Spectroscopy measurements from which clay content was calculated via a spectral library that is calibrated against the sieve and pipet method (NEN 5753:2018, 2018).

An ammonium oxalate (AO) extraction (ISO, 2012) was used for both soil sets to measure micro-crystalline Fe and Al, and P (Fe-AO, Al-AO, P_t-AO). Iron (Fe-D) and Al (Al-D) were also measured in a sodium-dithionite extraction (for the Dutch soils as described by Hiemstra et al., 2010a; for the Burundian soils as described in ISO, 2012), and crystalline Fe and Al were calculated as the difference between the Fe and Al measured in the dithionite and AO extraction. The Fe, Al and P_t in ammonium oxalate and Fe and Al in the dithionite extractions were analyzed using Inductively coupled plasma optical emission spectrometry (ICP-OES, iCAP6500, Thermo Scientific). The P_t measured in AO extraction can include phosphorus species that are different from inorganic PO_4, such as organic P (Jørgensen et al., 2015; Wolf and Baker, 1990). The latter is expected to not control the inorganic PO_4 concentration in the $CaCl_2$ extraction. Therefore, for the Burundian soils, the inorganic PO_4 concentration in the AO was measured using the molybdenum blue method (Murphy and Riley, 1962), using an SFA-PO_4 instrument. The samples were diluted 100 times with ultra-pure water to eliminate the interference of oxalate for the colorimetric reaction (Cui and Weng, 2013; Hass et al., 2011). For the Dutch soils, PO_4 was not measured in the AO extraction, but instead, an empirical relation was used to calculate the contribution of organic P species to the P_t measured in the AO based on the OC content in the soils (Mendez et al., 2020).

The humic and fulvic acid fractions of the organic matter in the solid phase were measured following the procedure as described by Van Zomeren and Comans (2007). The soils were extracted with ~0.1 M HCl (pH 1), after which the pellet was re-dissolved in ~0.1 M NaOH (pH 12). Subsequently, the supernatant of the acid extraction and the supernatant of the acidified base extract were combined and equilibrated with pre-cleaned DAX-8 resin. The fulvic acids were afterwards desorbed from the resin with 0.1 M KOH. The HA were measured by re-dissolving the pellet in the acidified base extract with 0.1 M KOH.

In addition, total boron content was measured in the soils. Soil digestion was done with a mixture of HNO_3–$HClO_4$–HF, in a ratio of 90:5:5, under heating at 190 °C for 10 h. Element concentrations of B, Si, Fe and Al were measured using ICP-OES.

2.2. pH dependent B solubility

The B–$CaCl_2$ concentration in the 10 soils was measured at different pH($CaCl_2$) levels, to assess the pH dependent B solubility. Two grams of soil was put into 50 ml polypropylene centrifuge tubes, together with 10 ml of 0.02 M $CaCl_2$ and 8 ml of ultra-pure water (UPW). The pH was adjusted through addition of 0.5 M HNO_3/NaOH. After 2 h, the pH was checked and more acid or base was added to obtain the pre-determined pH value. The same was done after 6 h, and ultra-pure water was added in order to reach a total volume of 20 ml with a final $CaCl_2$ concentration of 0.01 M. After 24 h, the final pH was measured, and samples were centrifuged and filtered over a 0.45 µm filter for the analysis of B on HR-ICP-MS, and TOC/IC on the SFA.

2.3. Reactive B extractions

Three different extraction methods were tested to estimate the geochemically reactive fraction of B in the soils. For all three soil extractions, no glassware was used throughout the extraction procedure to avoid B contamination.

Firstly, samples were suspended in a freshly prepared extraction solution with 0.05 M KH_2PO_4 at a SSR of 20. The suspensions were shaken for 16 h, and afterwards centrifuged and filtered over a 0.45 µm membrane filter. The protocol was based on the design by Hou et al. (1995), who used this extraction solution as part of a fractionation scheme, to quantify specifically bound B in soils on surfaces with variable charge. The B concentration in the blanks (n = 2) was negative.

Secondly, a 0.43 M HNO_3 extraction solution was used, with a SSR of 10 and an equilibration time of 4 h, according to the ISO standard (ISO, 2016). After centrifugation, the samples were filtered over a 0.45 µm membrane filter. The B concentration in the blanks (n = 4) was negative. This ISO protocol has been developed for measuring the reactive content of trace elements in the environment, and has been evaluated for a wide range of elements based on multi-surface modeling (Groenenberg et al., 2017). However, B was not included in that study, and the 0.43 M HNO_3 extraction is therefore evaluated here for its suitability to measure reactive B.

Thirdly, we used a mannitol extraction to estimate reactive B. Bingham (1982) formulated an extraction protocol to measure B by using 0.01 M mannitol + 0.01 M $CaCl_2$ solution. However, Goldberg and Suarez (2014) showed that the addition of Ca in the extraction solution resulted in a lower B concentration. The Ca was not included in their optimal extraction solution, since Goldberg and Suarez (2014) argued that the only reason to include Ca is to facilitate filtration because of coagulation of organic matter. Vaughan and Howe (1994) found that mannitol had similar effectiveness in extracting B as sorbitol, another polyol, when buffering the pH at 7.3 in both extraction solutions. A mannitol and sorbitol extraction is based on the principle of complex formation between the polyol and borate (Knoeck and Taylor, 1969). Borate ($B(OH)_4^-$) is the anionic form of B that is formed according to the reaction (Bassett, 1980):

$$B(OH)_3^0 + H_2O \Leftrightarrow B(OH)_4^- + H^+ \qquad logK = -9.24 \tag{1}$$

The complexation of mannitol with boron then proceeds according to the reactions (Knoeck and Taylor, 1969):

$$B(OH)_3^0 + H_2O + Mannitol \Leftrightarrow B(OH)_4^- - Mannitol + H^+ \quad logK = -6.45 \tag{2}$$

$$B(OH)_3^0 + H_2O + 2Mannitol \Leftrightarrow B(OH)_4^- - Mannitol_2 + H^+ \quad logK = -4.26 \tag{3}$$

with the latter being the most important species. The formation of borate is only significant at high pH values. Since the polyol forms complexes with borate (Knoeck and Taylor, 1969), the pH of the extraction solution affects the concentration of borate and thus the final B measured in the extract (Aitken et al., 1987). In this study, the extraction was executed with a mannitol concentration of 0.2 M, together with 0.1 M triethanolamine (TEA) buffer (pH 7.3), with an equilibration time of 24 h and a SSR of 10. This concentration, equilibration time and SSR were suggested by Goldberg and Suarez (2014) for their optimal sorbitol extraction. The samples were filtered over a 0.45 µm filter after centrifugation. The average B concentration of the blanks (n = 2) was 0.01 ± 0.008 mg L^{-1}.

For the mannitol extraction, the B was measured using ICP-OES. For the HNO_3 extraction, ICP-OES was used for the Dutch soils, and HR-ICP-MS for the Burundi soils. For the B measurement in $CaCl_2$ and KH_2PO_4, HR-ICP-MS was used. The concentrations of Si, Fe and Al in the three extractions was measured using ICP-OES, to assess the potential dissolution of minerals that could contain B.

2.4. Multi-surface modeling set-up

The multi-surface model included ion adsorption to organic matter, the edges of clay minerals and Fe and Al (hydr)oxides. For adsorption to the reactive surfaces, we used specific models for each surface. The aqueous species are given in Table S1 in the supporting information. All modeling and adsorption parameters are given in Tables S2–S3. Modeling calculations were performed in ECOSAT, version 4.9 (Keizer and Van Riemsdijk, 1995).

2.4.1. Oxides

The CD-MUSIC model was used to model adsorption to oxides. The content of poorly crystalline oxides was calculated based on the Al and Fe found in AO extraction. To transform the moles of Al and Fe in the AO extraction to the oxide mass, a molar mass of 95 g mol^{-1} Fe and 84 g mol^{-1} Al was used, which corresponds to particles with a specific surface

area of 600 m^2 g^{-1} (Hiemstra and Van Riemsdijk, 2009). The amount of crystalline oxides was calculated based on the difference between the Fe and Al in the sodium-dithionite extraction and the Fe and Al measured in the ammonium-oxalate extraction, with a molar mass of respectively 89 and 78 g mol^{-1} for Fe (goethite) and Al (gibbsite) (Hiemstra et al., 2010). For the crystalline oxides, a specific surface area of 100 m^2 g^{-1} was assumed (Dijkstra et al., 2009). Ferrihydrite (Fh) was used as model oxide for the natural oxide fraction of the soils. The total Fh content was calculated by summing the mass of poorly crystalline oxides and 1/6 of the mass of crystalline oxides, and in the modelling calculations a specific surface area of 600 m^2 g^{-1} was used for Fh.

Next to $B(OH)_3$, adsorption of H^+, Ca^{2+}, Cl^-, CO_3^{2-} and PO_4^{3-} on the oxide surface was included in the model. The B binding on oxide surfaces is pH dependent. Competitive anions such as PO_4^{3-} and CO_3^{2-} can reduce the B binding to oxides (Van Eynde et al., 2020; Xu and Peak, 2007). Binding of both ions is affected by the Ca^{2+} and Cl^- ion adsorption due to mainly electrostatic effects and additional surface species. The Ca^{2+}, CO_3^{3-} and Cl^- concentrations in the $CaCl_2$ extraction, and the inorganic PO_4 in the AO extraction were given as input for modelling B speciation. For modeling the adsorption of these ions to ferrihydrite, a consistent set of recently derived adsorption parameters was used (Hiemstra and Zhao, 2016; Mendez and Hiemstra, 2018, 2020a, 2020b; Van Eynde et al., 2020) which is shown in Table S2.

In addition, experiments have shown that soil organic matter can be a competitor with B for adsorption on the oxide surface (Marzadori et al., 1991; Sarkar et al., 2014). To account for this effect, we have used the modelling approach from Hiemstra et al. (2013) to calculate the natural organic matter (NOM) loading on the oxide surface. The NOM surface species with corresponding charge distribution and log*K* values are given in Table S2. Before modelling B speciation, the NOM loading was fitted for each soil sample based on the PO_4 solid-solution partitioning. In these modelling calculations, the inorganic PO_4 in the AO extraction was given as input, together with the pH($CaCl_2$), the CO_3^{2-}, Ca^{2+} and Cl^- concentration in the $CaCl_2$ extraction, the content of clay minerals and Fh. The NOM loading was adjusted until the calculated dissolved PO_4 corresponded to the measured PO_4 concentration in the $CaCl_2$ extraction, and this NOM loading was further used in modelling the B speciation. The results from this modelling calculation for the different soils are given in Table S4.

The effect of including the different competitors for B adsorption on oxides, i.e. NOM, CO_3 and PO_4, on the modelling calculations is shown in Fig. S1 in the supporting information.

2.4.2. Organic matter

Adsorption to organic matter was modelled by using the NICA-Donnan model (Kinniburgh et al., 1996), assuming that the interaction between oxides and organic matter does not influence the B adsorption to the organic matter. We considered the reactive organic matter as humic acids, since NICA parameters are only available for B adsorption on humic acids (Goli et al., 2019). For the dissolved organic matter, 50% was considered as humic acids for both Dutch and Burundian soils as it has been done previously (Dijkstra et al., 2009; Groenenberg et al., 2017). The solid humic acids were calculated as the sum of the fulvic and humic acids that were measured according to the batch procedure of Van Zomeren and Comans (2007). Next to B, we considered adsorption of H^+ and Ca^{2+} on humic acids. Goli et al. (2019) showed that next to pH, the B binding to HA is affected by the presence of Ca^{2+} due to site competition and electrostatics. Except for the model parameters for B, all other NICA-Donnan parameters are based on the generic parameters for humic acid from Milne et al. (2003) including the site densities of the carboxylic and phenolic groups, as well as the b-parameter to calculate the Donnan volume based on ionic strength (Table S3).

The NICA-Donnan model calculates total ion adsorption as the sum of the specifically and electrostatically adsorbed concentrations, with the latter being the Donnan species in the Donnan layer of the humic acids. For the neutral $B(OH)_3^0$ ion, which is the dominant ion in the pH range of these soil samples (Eq. (1)), there is no electrostatic attraction. Therefore, we did not include the $B(OH)_3^0$ present in the Donnan layer for calculating the total adsorbed B to humic acids. Calculations showed that the contribution of the electrostatically bound B as Donnan species to total B adsorbed to humic acids in the $CaCl_2$ extraction was less than 10%.

2.4.3. Clay

In previous multi-surface modeling studies, ion adsorption to clay minerals has been considered as an electrostatic process, which has been modelled using a Donnan approach (Dijkstra et al., 2009; Weng et al., 2001). Since B will be present in solution mainly as a neutral species (Eq. (1)), there will be no electrostatic attraction/repulsion. However, B can bind to the reactive surface sites on the edges of clay minerals. Therefore, we included specific B adsorption to the edges of the clay surfaces. The content of clay minerals was estimated as the measured clay content (i.e. particles smaller than 2 μm) minus the mass of oxides that were calculated as described above.

We assumed that the B adsorption behavior on clay edges can be modelled using the CD-MUSIC modeling parameters for ferrihydrite. This was tested by using the B adsorption parameters for ferrihydrite from Van Eynde et al. (2020) for describing the pH dependent B adsorption to illite and kaolinite clays from Goldberg (1999), assuming an SSA of 15 and 5 m^2 g^{-1} respectively. The results are shown in Fig. S2. The pH dependent B adsorption to clays can be described reasonably well with the parameters for ferrihydrite, especially for kaolinite. These results are consistent with the findings of Goldberg (1999) that the log*K* values for pH-dependent B adsorption, fitted by using the CC model, did not differ significantly for iron oxides and clay minerals such as kaolinite and illite.

For the multi-surface modelling calculations, it was assumed that next to $B(OH)_3$, adsorption of H^+, Ca^{2+}, Cl^-, CO_3^{2-} and PO_4^{3-} to these clay edges can be also described using the consistent set of adsorption parameters for ferrihydrite (Hiemstra and Zhao, 2016; Mendez and Hiemstra, 2018, 2020a, 2020b) as presented in Table S2. No interaction of NOM with the clay minerals was considered, based on previous findings that have shown that organic matter is mainly associated with the micro-crystalline oxide fraction in soils (Mendez et al., 2020).

An (edge) specific surface area of 5 m^2 g^{-1} was considered in the modelling calculations (Heidmann et al., 2005) since we did not have knowledge on the specific clay minerals being dominant in the different soil samples. Although the 5 m^2 g^{-1} might be an underestimation of the edge surface area for clays such as illite, the modeling results were not greatly affected by the chosen edge surface area of the clay minerals (Fig. S3).

2.5. Multi-surface modeling calculations

We firstly calculated the reactive B for the ten soil samples using a multi-surface model with the B measured in the $CaCl_2$ at the original soil pH($CaCl_2$) as input. Because in the ECOSAT speciation software, only free ion concentration/activity or total amount of a compound can be used as the input, this calculation was carried out in two steps. Firstly, free $B(OH)_3$, CO_3^{2-}, Ca^{2+} and Cl^- concentrations were calculated based on the measured B concentration in $CaCl_2$ extraction considering solution speciation and B and Ca adsorption to DOC. Secondly, the calculated free ion concentrations of $B(OH)_3$, CO_3^{2-}, Ca^{2+} and Cl^- were used as input together with pH($CaCl_2$), PO_4-AO as reactive PO_4 and the reactive surfaces (including DOC), to model the solid and solution distribution of B. The NOM loading at the oxide surface, which was derived by preliminary modelling of the PO_4 solubility, was also given as input. From these modelling calculations, the B distribution over the different solid and solution phases could be extracted, and the total reactive B concentration was then calculated as the sum of soluble and adsorbed B.

The calculated reactive B was subsequently compared with the B measured in the HNO_3, KH_2PO_4 or mannitol extraction to assess the

suitability of the different extraction methods to measure reactive B in soils (Section 3.2). For this purpose, we calculated the mean error (ME) as the mean difference between the predicted and measured concentrations (in log mol kg^{-1}).

Additionally, we tested the capacity of the different extraction methods to dissolve reactive B, by modeling the solid and solution distribution of B in the respective extraction method. Following the approach of Groenenberg et al. (2017), we accounted for the adsorption of B to the major reactive mineral (oxides and clay) and organic adsorbents in the soil as described above, and the chemical composition of the specific extract, including (1) pH of the extractant (7.3 for mannitol; 0.9 for 0.43 M HNO_3 (Groenenberg et al., 2017); 4.5 for KH_2PO_4), (2) concentration of the major dissolved ions in the extraction solution (0.43 M NO_3; 0.05 M K; 0.2 M mannitol, respectively). The reactive B calculated based on the B measured in the 0.01 M $CaCl_2$ at natural pH ($CaCl_2$), was used in the model as input for total reactive B. The capacity of the different extraction methods for extracting B was calculated as the percentage of total B input that was predicted to remain in solution according to the model.

The input of total reactive P for the KH_2PO_4 solution was given as the sum of the PO_4 in the acid ammonium oxalate extraction and the 0.05 M PO_4 from the extraction solution. For the HNO_3 and mannitol extraction, input of total reactive PO_4 was given as the PO_4 in the ammonium oxalate extraction. The ionic strength of the mannitol extraction was fixed at 0.05 M, based on the presence of H-TEA^+ of around 50% of total TEA (Scopes, 1994). In the HNO_3 extraction, the oxide surface for ion adsorption will be reduced due to partial dissolution of the poorly crystalline oxides at pH 0.9. This was taken into account, by subtracting the Fe and Al concentration in the HNO_3 extractions from the concentrations in the AO extraction to calculate the oxide content. No competition of NOM for B adsorption to oxides in the different extractions was considered in this modelling calculations.

Preliminary modeling has shown that the presence/absence of measured DOC concentration did not lead to differences in the calculated extractability of the different extraction methods (Results not shown). Therefore, DOC was not included as a reactive surface in these calculations.

In a final modeling calculation, calculated concentration of B in solution was compared with the measured data of the pH dependent B solubility experiment. In this calculation, reactive B, pH, total reactive PO_4^{-3}, concentration of CO_3^{2-}, Ca^{2+} and Cl^- in the extractant, total reactive surfaces (including DOC) were used as input. The NOM loading that was calculated based on modelling the PO_4 solubility at the original soil pH($CaCl_2$) was used as input. The input value for reactive B was either the one calculated based on the B measured in $CaCl_2$ extraction at natural soil pH, or the B measured in each of the extraction methods (i.e. HNO_3, KH_2PO_4, mannitol).

3. Results and discussion

3.1. Soil characteristics

Soil characteristics of the Dutch (D1-5) and Burundian soils (B1-5) are given in Table 1. The Dutch soils have higher B concentrations than the Burundian soils, in all extraction methods, except for soil D2 which has low total boron relatively to the other Dutch soils. In general, the tropical soil samples from Burundi are characterized by higher contents of oxides, more specifically oxalate-extractable Al and dithionite-extractable Fe. The pH of the Burundian soil samples is similar for all samples, between 4.2 and 4.9, whereas for the Dutch soils, the pH ranges from 4.7 to 7.1.

Total B is higher than the B concentrations found in the other extractions. The fraction of total B found in the extractions used to measure reactive B ranges from 2 to 5%, depending on the extraction method. Highest B concentrations are found in the HNO_3 and mannitol extractions, followed by KH_2PO_4 and $CaCl_2$. The fraction of reactive B that is found in the $CaCl_2$ extraction can be used as an indicator of the adsorption capacity of the soils, and this fraction is on average 42, 51 and 77% when using respectively the B measured in HNO_3, mannitol and KH_2PO_4 as reactive B. In two cases, the $CaCl_2$ has extracted slightly more B than the KH_2PO_4 solution (i.e. D3 and B3). The B concentrations in all extractions were found to be significantly correlated among each other (Table S5).

The observed B concentrations in the $CaCl_2$ extraction as a function of pH cannot be explained by the solubility of B-containing Ca, Mg and Na minerals, such as Pinnoite, Inderite, Colemanite, Inyoite, Borax, McAllisterite and Nobleite (Parks and Edwards, 2005). The solubility of B based on these minerals differ orders of magnitude from our observations, and show a reverse pH trend from what we have found here. These observations are consistent with the findings from Fruchter et al. (1990) who did not find B solubility-controlling phases in waste material.

The risk of boron deficiency is often estimated by a hot water soil extraction (Sparks et al., 1996). Critical B concentrations in hot water extractions for crop production are reported to be in the range of 9–28 μmol kg^{-1} for acidic and neutral soils (Kabata-Pendias and Pendias, 2001). Novozamsky et al. (1990) established a relation between B measured by hot water and 0.01 M $CaCl_2$ extraction for 100 soils from

Table 1
Soil characteristics. HA and FA are the humic and fulvic acids measured in the acid-base fractionation of the solid organic matter. The P_t-AO, Fe-AO and Al-AO are measured in ammonium oxalate, whereas Fe-D and Al-D are measured in dithionite extraction. B was measured in 0.43 M HNO_3, 0.05 M KH_2PO_4, 0.2 M mannitol and 0.01 M $CaCl_2$. The B-reactive is the reactive B calculated with the multi-surface model using the B–$CaCl_2$ as input.

Soil	pH	Clay	SOC	HA+FA	DOC	Fe-AO	Al-AO	Fe-D	Al-D	P_t-AO	B-total	B-HNO_3	B-KH_2PO_4	B-Mannitol	B-$CaCl_2$	B-Reactive
		%	g C kg-1		mg L^{-1}	mmol kg^{-1}					μmol kg^{-1}					
D1[A]	7.1	24	20	2	22	27	17	141	27	12.24	5943	480	274	271	77	85
D2[A]	4.8	3	32	15	43	37	42	38	39	13.53	773	81	41	43	40	45
D3[A]	4.7	11	133	*49**	131	136	89	107	63	26.38	**	166	61	**	77	101
D4[A]	5.8	35	31	9	36	89	21	164	24	21.15	6090	332	162	156	85	100
D5[A]	6.4	39	85	21	105	133	44	192	29	33.23	5950	393	142	188	72	106
B1[B]	4.3	7	50	25	11	156	314	456	328	11.43	1754	29	23	38	20	28
B2[B]	4.4	10	28	10	9	71	168	493	244	7.52	1097	39	25	36	24	30
B3[B]	4.3	17	22	12	10	58	147	647	253	3.91	568	14	7	16	7	9
B4[B]	4.2	4	14	5	5	37	63	616	139	3.36	778	15	8	18	7	8
B5[B]	4.9	8	32	15	3	66	136	328	171	4.00	1165	33	18	32	13	16

* Insufficient soil material was left for this analysis. Therefore, the average % of total OC that was found to be HA and FA for the other soil samples was taken as reactive OC. This was 30% HA and 6% FA.
** Insufficient soil material was left for this analysis. This sample was not included in the discussion of the mannitol extraction.
A Temperate soil samples from the Netherlands
B Tropical soil samples from Burundi

the Netherlands, and they found that ~ 26% of B measured by hot water is extracted by the $CaCl_2$ extraction. This would mean a critical concentration of ~7 μmol kg^{-1} of B in 0.01 M $CaCl_2$. As can be seen in Table 1, the B measured in $CaCl_2$ is higher than this critical value except for soil B3 and B4.

3.2. Reactive B

Based on the B measured in 0.01 M $CaCl_2$ in soils at their original soil pH($CaCl_2$), the total reactive B was calculated by the multi-surface model as the sum of adsorbed and soluble B. The results of these calculations for each soil sample are shown in the last column of Table 1.

We tested the capacity to dissolve reactive B for the three different extraction methods. Multi-surface modelling calculations of boron speciation in the different extraction solutions show that more than ~90% of the reactive boron from Table 1 is dissolved by each of these solutions (Fig. S4). The three different extraction solutions from this study are thus, based on these modeling calculations, efficient in extracting reactive boron from soils.

A 0.43 M HNO_3 solution extracts metal cations by competitive desorption with protons and it dissolves oxyanions due to their protonation at low pH and partial dissolution of hydrous oxides to which anions are adsorbed (Groenenberg et al., 2017). Van Eynde et al. (2020) showed that at low pH, oxides, and especially ferrihydrite exhibit larger adsorption affinity for B compared to organic matter. The model predicts that still up to 10% B is adsorbed to ferrihydrite, at pH 0.9 in the 0.43 M HNO_3 extract (Fig. S4).

Similar results for boron speciation are found for the KH_2PO_4 and HNO_3 extraction. The KH_2PO_4 extraction method is a milder extraction solution in terms of pH (4.5), but adds in turn a strong competing phosphate ligand to desorb the B from the solid phase (Chao and Sanzolone, 1989; Hou et al., 1995). Fig. S4 shows that for the soils with the highest organic matter and ferrihydrite content (B1 and D3), part of the boron is not in solution but is predicted to be adsorbed to oxides and organic matter.

The addition of 0.2 M mannitol to the soil samples results in nearly 100% of all reactive boron in solution (Fig. S4), according to the complexation constants from Knoeck and Taylor (1969) (Equations (2) and (3)). Only the reaction of mannitol with $B(OH)_3$ was included in the modelling. However, it is known from literature that mannitol can also form complexes with other anions and cations (Bourne et al., 1961; Doleźal et al., 1973; Kutus et al., 2017), but no consistent log*K* values for complex formation with the uncharged mannitol are reported. The presence of other cations and anions in the soil system might therefore reduce the actual recovery of B by a mannitol extraction.

Fig. 1 shows the comparison between calculated reactive B with the multi-surface model, and the actual B concentrations measured in the three different extraction solutions. Although the model predicts that all three extraction methods are efficient in dissolving reactive B (Fig. S4), Fig. 1 shows that for most soils more B is extracted than the amount of reactive B according to the multi-surface model.

For the temperate soils, the HNO_3-extractable B deviated most from the prediction, followed by B in the mannitol and in KH_2PO_4 extracts, with ME of −0.46, −0.23 and −0.12 respectively. For the tropical soils, the KH_2PO_4 extraction also gave the best results with a ME of 0.04. Using the mannitol and HNO_3 extraction resulted in a ME of −0.22 and −0.18 respectively and both extraction methods result in an over-estimation of reactive B for all tropical soil samples.

As shown in Fig. 1, the measured B–HNO_3 is larger than the reactive B predicted for all soil samples. The measured B concentration in HNO_3 is on average 240% of the calculated reactive concentration, indicating that 0.43 M HNO_3 has dissolved non-adsorbed B. A 0.43 M HNO_3 extraction acidifies the soils to a pH between 0.5 and 1, which can result in a dissolution of various minerals, including Fe oxides and silicate minerals (Groenenberg et al., 2017; Huertas et al., 1999). Since most of the total soil B can be a structural part of clay minerals (Hou et al., 1994; Lemarchand et al., 2012), this nitric acid extraction can solubilize non-reactive B. The B in the HNO_3 differs more from the calculated reactive B for the Dutch than for the Burundian soil samples. This difference might be explained by the difference in soil pH, degree of weathering and clay type: The tropical Burundian soils have a relatively low pH compared to the Dutch soils, therefore the minerals present in the Dutch soils are more sensitive to acid extraction. In addition, the tropical Burundian soils are likely dominated by clay minerals such as kaolinite, due to prolonged intensive weathering, while illite-type clays are more representative for the less weathered temperate Dutch soils. Illite releases higher absolute concentrations of Si than kaolinite in acidic solutions (Bibi et al, 2011, 2012; Lindsay, 1979) and has been found to have a slightly higher dissolution rate at an acidic pH, compared to kaolinite (Köhler et al., 2003). In addition, illite contains more B than kaolinite (Couch, 1971), which, next to the larger amount of clay minerals dissolved, might contribute to the higher ME for the Dutch soils when comparing the predicted reactive B with the B measured in HNO_3.

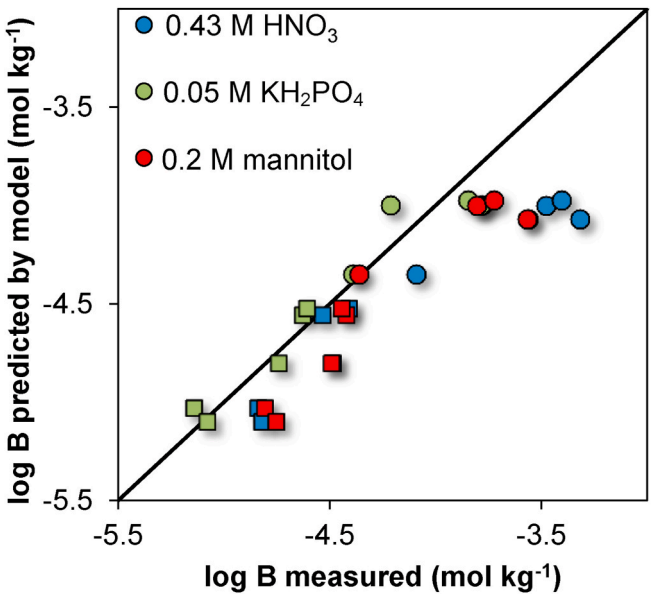

Fig. 1. Comparison between the B measured in HNO_3, KH_2PO_4 or mannitol with the B that is calculated by the model from soluble B in $CaCl_2$ as total reactive B based on adsorption processes on humic acids, clay minerals and ferrihydrite for the different soil samples. The Dutch soils are shown by circles, the Burundian soil samples by squares and the color of the markers shows the different extraction for the B measurement. The corresponding mean error based on log mol kg^{-1} concentrations are −0.32 for HNO_3 (−0.46 for temperate, −0.18 for tropical), −0.04 for KH_2PO_4 (−0.12 for temperate, 0.04 for tropical), −0.22 for mannitol (−0.23 for temperate and −0.22 for tropical). (For interpretation of the references to color in this figure legend, the reader is referred to the Web version of this article.)

For the temperate soil samples, mannitol results in a slightly more negative ME compared to KH_2PO_4, and both extractions overestimate reactive B with extracted concentrations being on average 177% and 123% of the predicted reactive B respectively. For the tropical soils the mannitol extraction also overestimated reactive B (on average 170%) compared to predictions by the multi-surface model (Fig. 1), and unlike for the temperate soils, the B extracted by mannitol is even slightly higher than the B extracted by 0.43 M HNO_3. In line with the B measurements, mannitol extracts the largest fraction of total Si, Al and Fe in most of the tropical soil samples (Table 2). Although the samples extracted with mannitol were filtered over a 0.45 μm filter before analysis, the high B, Si, Al and Fe concentrations in the mannitol extraction can be an indication of colloidal particles (<0.45 μm) in the extract because of the low salt level in the mannitol extraction. Although

Table 2
The Si, Al, Fe and B measured in the soil digestion and the HNO_3, KH_2PO_4 and mannitol extraction of the Dutch (D1-5) and Burundian soils (B1-5). The bold numbers show that Si in HNO_3 is relatively high for the temperate soils (D1-5), while for the tropical soils (B1-5) in mannitol. The same holds for Fe. Al is highest in HNO_3 for temperate soils, and in both extractions for the tropical soils.

	Si				Al				Fe				B			
	Total	HNO_3	KH_2PO_4	Mannitol	Total	HNO_3	KH_2PO_4	Mannitol	Total	HNO_3	KH_2PO_4	Mannitol	Total	HNO_3	KH_2PO_4	Mannitol
	mol kg^{-1}	mmol kg^{-1}			mol kg^{-1}	mmol kg^{-1}			mol kg^{-1}	mmol kg^{-1}			mmol kg^{-1}			
D1	11.80	**50.78**	0.34	2.20	1.90	**33.47**	0.09	0.07	0.44	**26.36**	0.03	0.05	5.94	0.48	0.27	0.27
D2	13.37	**-**	0.06	2.60	0.96	**97.59**	2.53	6.38	0.09	**21.94**	0.25	1.61	0.77	0.08	0.04	0.04
D3	–	**4.43**	0.06	–	–	**178.63**	2.90	–	–	**74.81**	0.42	–	–	0.17	0.06	–
D4	11.27	**40.18**	0.29	7.05	5.06	**106.48**	0.89	6.85	0.50	**60.04**	0.15	1.06	6.09	0.33	0.16	0.16
D5	8.84	**27.43**	0.32	18.34	5.70	153.28	2.85	27.57	0.50	**54.10**	0.32	2.27	5.95	0.39	0.14	0.19
B1	8.52	21.06	0.33	**30.16**	9.19	**586.40**	5.31	91.77	0.61	**20.68**	0.27	6.68	1.75	0.03	0.02	0.04
B2	10.26	18.57	0.31	**30.91**	7.59	**297.04**	5.31	122.48	0.76	**12.62**	0.37	**12.71**	1.10	0.04	0.02	0.04
B3	9.37	12.60	0.32	**115.65**	8.24	224.88	5.92	**414.62**	0.98	7.65	0.39	**44.19**	0.57	0.01	0.01	0.02
B4	11.89	6.52	0.19	**58.57**	2.61	101.85	3.29	**162.44**	0.36	4.87	0.16	**15.99**	0.78	0.02	0.01	0.02
B5	7.89	32.36	0.48	**42.12**	10.65	**252.64**	1.22	123.68	1.19	5.41	0.04	**9.92**	1.16	0.03	0.02	0.03

the ionic strength was not measured in the mannitol extraction, it was possibly lower in the extracts from the tropical soils, due to a lower concentration of charged ions because of prolonged weathering. Moreover, the larger increase in pH relative to the original soil pH upon addition of the (buffered, pH 7.3) mannitol extraction solution for the tropical soils, can also favor the formation of colloids in the extract (Kaplan et al., 1996; Kretzschmar and Sticher, 1998).

Additionally, the ligands in the mannitol extraction (mannitol, TEA buffer), can form soluble complexes with Si, Al and Fe, thus enhancing the solubility of B-containing minerals at alkaline pH. Kinrade et al. (1999) found that poly-hydroxy alcohols, such as mannitol and sorbitol, another commonly used polyol for B extraction (Goldberg and Suarez, 2014), form concentrations of stable complexes with silicate anions. Moreover, these authors reported that the Si complexation with polyols enhances silica solubility. It has also been shown that mannitol can form complexes with metals (Doleźal et al., 1973), such as Fe (Doleźal and Langmyhr, 1972). Similarly, the use of TEA buffer might also lead to enhanced Fe and Al mineral dissolution, since it has been reported that TEA can form stable complexes with Fe in alkaline solutions (Mohr and Bechtold, 2001) as well as with Al (Karlsson et al., 2009), which can possibly lead to dissolution of Fe/Al minerals. Since the TEA buffer is also a typical component of the frequently used DTPA extraction for measuring bioavailable Fe (Lindsay and Norvell, 1978), this possible effect on mineral dissolution may be worth further investigation.

Modifications in the extraction protocols, such as shorter equilibration time, lower concentration of mannitol or increasing the salt level of the extraction, might reduce the risk of dissolution, or formation of colloids, of non-reactive B. Measurements of Si, Al and Fe should thus be included in experiments testing different extraction protocols, to assess possible mineral dissolution, colloid formation, and associated mobilization of non-reactive B.

Overall, the KH_2PO_4 is the best extraction method to quantify reactive boron for both tropical and Dutch soils (Fig. 1). For soils D2, D3, B1, B2 and B3, there seems to be either an under-estimation of reactive B by the KH_2PO_4 extraction or an over-estimation of B adsorption by the multi-surface model. However, the differences between B–KH_2PO_4 and calculated reactive B are relatively small (Table 1). These soils are characterized by a low pH and a high content of organic matter and ferrihydrite. Using the multi-surface model to calculate the B speciation in the KH_2PO_4 extraction has shown that B was still partly bound to organic matter and ferrihydrite for these soils (Fig. S4). A twofold increase in PO_4 concentration in the extraction solution would still lead to a fraction of B that is bound to oxides instead of being extracted (results not shown).

For soils D1, D4 and D5, either the KH_2PO_4 solution extracts more B than is predicted by the model to be reactive, or the model underestimates adsorption for these samples. These are the soil samples with the highest clay content and highest pH. The B adsorption to clay particles was modelled using the adsorption parameters for ferrihydrite and a surface area of 5 $m^2\ g^{-1}$. The latter could be an under-estimation of the actual specific surface area but changing the SSA of the clay edges did not have a large effect on the calculations (Fig. S3). Another explanation might be that the KH_2PO_4 extraction potentially solubilizes part of the B that is occluded in the clay minerals (Gaillardet and Lemarchand, 2018; Hou et al., 1994), however, this is unlikely at the pH 4.5 of this extraction. The Si measured in the KH_2PO_4 extraction for soils D1, D4 and D5 is higher than for the other Dutch soils (Table 2), which might be due to competition with adsorbed Si by the added PO_4 (Hiemstra, 2018). Additionally, the multi-surface model might under-estimate B adsorption in these high pH soils. The model performance in describing pH dependent B solubility is further discussed in Section 3.4.

3.3. Boron speciation in soils

Based on the B measured in 0.01 M $CaCl_2$, the geochemical reactive B

was calculated. In addition, from this modelling calculation the distribution of B over the solid and solution phase can be obtained. This predicted B speciation for the 10 soil samples is shown in Fig. 2. The model predicts that most of the geochemical reactive B is in the solution phase, with a minimum of 68% for soil D5. The adsorption to dissolved organic matter is negligible and maximal 1% of boron in solution was calculated to be bound to DHA. This finding is consistent with previous studies that have shown that B is mainly present as free dissolved B instead of being bound to dissolved organic matter (Pédrot et al., 2008; Pokrovsky and Schott, 2002). From the inorganic aqueous species that were considered in the modelling (Table S1), $B(OH)_3^0$ was predicted to be most important, representing >99% of all B in solution.

Our modeling results show that the contribution of the reactive surfaces for boron adsorption is different for the tropical and temperate soils: in the temperate soils, organic matter contributes mainly to B adsorption, whereas oxides play the most important role in the tropical Burundian soils. The difference in solid phase B speciation between the temperate and tropical soils can be explained by pH, the amount of reactive surfaces and PO_4^{3-} loading. The tropical soils in our dataset are characterized by a low pH, and it has been shown that under these conditions ferrihydrite exhibits the largest B adsorption capacity of all reactive surfaces considered, according to the multi-surface model (Van Eynde et al., 2020). In addition, as shown in Fig. S1, the exclusion of PO_4 in the modelling led to a higher reactive B concentration calculated by the model, due to an increased B binding to oxides.

It has been previously shown that B amended to a variety of soil systems binds only weakly to the solid phase (Mertens et al., 2011). Fig. 2 shows that the same holds for the reactive B that is *in situ* present in soils. It has been stated before that the interaction of B with the soil solid phase controls the B in solution and consequently B bioavailability (Goldberg, 1997; Keren et al., 1985). However, the multi-surface modelling calculations show that the interaction of natural reactive B with the solid phase is limited, and that a substantial part of the bioavailable boron will be in the solution phase. Other processes than adsorption will therefore be more important for buffering bioavailable B in the soil solution. Next to atmospheric input via precipitation and aerosol deposition, two potential processes in soils might be important for B replenishment to the soil solution; B originating from mineral weathering (Su and Suarez, 2004), and from mineralization of organic matter that originates from plant material (Gaillardet and Lemarchand, 2018). Evidence for both processes have been found in previous studies. For example, isotopic measurements in forest stands have shown that the B in solution in the upper soil layers appears to be mainly originated from decomposing vegetation (Cividini et al., 2010; Lemarchand et al., 2012). On the other hand, a similar study showed that for two soil profiles rich in clay minerals the B behavior was not controlled by biological cycling but most probably by chemical weathering (Noireaux et al., 2014). Kot et al. (2016) measured B in leachates from litter and leaves, and found higher B concentrations and fluxes than the ones estimated from chemical weathering or atmospheric deposition for the global biogeochemical cycle of boron (Park and Schlesinger, 2002). They concluded that the turnover of organic inputs is the main source for bioavailable B in soils.

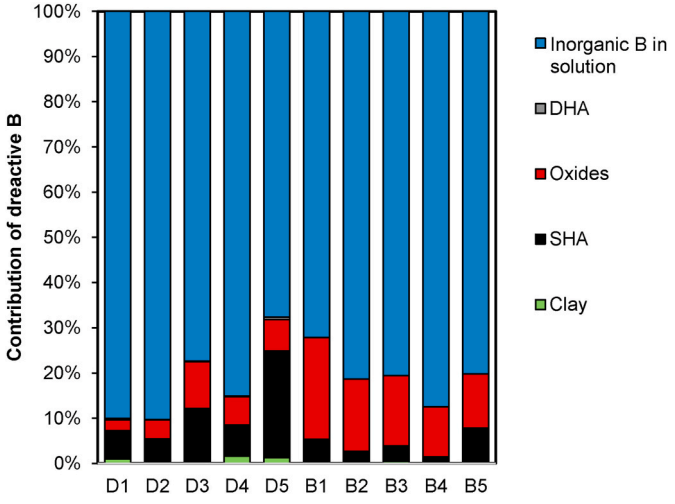

Fig. 2. B speciation in the 10 soil samples calculated by the multi-surface model based on the B measured in the 0.01 M $CaCl_2$ extraction. The B is distributed in the solution phase as inorganic B species (>99% as $B(OH)_3$) and bound to dissolved organic matter (as humic acid, DHA), and in the solid phase bound to oxides, solid organic matter (as humic acid, SHA) and Clay. The soils D1-D5 are the 5 Dutch soils, while soils B1–B5 are the 5 Burundian soils (soil properties are shown in Table 1).

The question arises how these results from forests stands can be translated to agricultural top soils, where above ground biomass is largely removed from the field after the growing season. Given that adsorption contributes only minor to the bioavailable boron pool and that both mineralization of organic matter and chemical weathering have been suggested as potential processes that resupply boron in the soil solution, we have performed a regression analysis between B concentrations in the $CaCl_2$ and the SOC and clay content of the soils. These results are shown in Fig. S5. For the Burundian soil samples, there is a tendency that the largest B in $CaCl_2$ is found for those soils with the highest organic carbon content, while this is not the case for the Dutch soils. For the latter, the relation between B in $CaCl_2$ and clay content seems to be more important. Even though organic matter represents the most important adsorption surface for the Dutch soils (Fig. 2), chemical weathering might be more important for buffering bioavailable boron. Although the regression was done based on a small set of soils (n = 5), these results can be indicative that different processes such as mineralization and chemical weathering can be important for buffering bioavailability of B in the different soil sets of this study.

3.4. Model performance to describe pH dependent B solubility in soils

Adsorption experiments on reactive surfaces have shown that B adsorption increases with increasing pH up to a maximum at around pH 8–10 (Goldberg and Glaubig, 1985; Lemarchand et al., 2005; Van Eynde et al., 2020). In line with these results, we found for all soil samples a decreasing B concentration in the 0.01 M $CaCl_2$ with increasing pH (Fig. 3). The decrease in B with increasing pH, calculated as $\Delta B/\Delta pH$ was between 0.1 (B4) and 6 μmol L^{-1} (D1) per unit of pH. Except for soil D1 and D4, the experimental data shows that the decrease in B concentration with increasing pH is related to the soil organic carbon content (Fig. S6). This is also predicted by the multi-surface model: a decrease in B concentration with increasing pH is due to an increase in B adsorption to soil organic matter (Fig. S7) and for soils with higher SOC, a larger decrease in B concentration with increasing pH is consequently predicted by the model.

Both modelling predictions and experimental data show that from pH > 6, more than 50% of reactive boron is in the solid phase, mainly adsorbed to solid organic matter (Fig. S7).

In Fig. 3, the dashed line (model 2) shows model calculations in which the B solubility was calculated with KH_2PO_4-extracted B as input for reactive B. The latter was chosen since the B in this extraction method differed the least from the calculated reactive B by the model (Fig. 1). In terms of absolute prediction levels with KH_2PO_4–B as input, it can be seen that for some soils the B concentrations in the $CaCl_2$ extraction are over-estimated by up to a factor of 5 (D1), and for some soils under-estimated by up to a factor of 2 (D3).

In order to assess model performance irrespective of the chosen extraction method, the pH dependent B solubility was calculated using as input the reactive B as it was calculated based on the B measured in 0.01 M $CaCl_2$ at the original soil pH. This is shown as the solid line (model 1) in Fig. 3. Looking at these modeling calculations, it can be

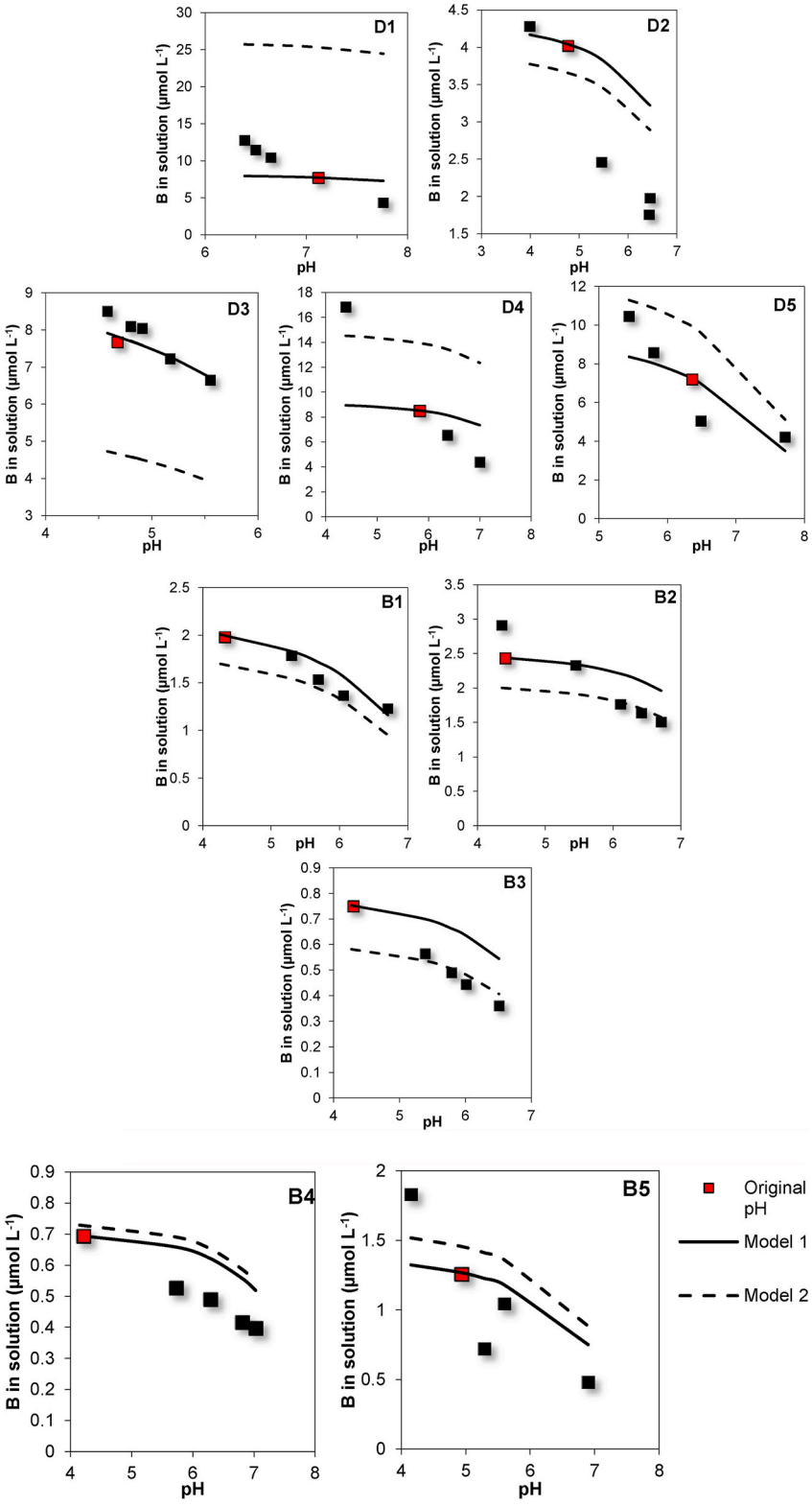

Fig. 3. pH dependent B concentration for all 10 soil samples. Red markers show B concentration at natural soil pH. B and pH were measured in 0.01 M $CaCl_2$ after 24 h. Modeling calculations were performed using either the calculated reactive B based on the measured B in $CaCl_2$ at original pH ($CaCl_2$) (Model 1) or using the B measured in 0.05 M KH_2PO_4 as input for reactive B (Model 2). The soils D1-D5 are the 5 Dutch soils, while soils B1–B5 are the 5 Burundian soils (soil properties are shown in Table 1). (For interpretation of the references to color in this figure legend, the reader is referred to the Web version of this article.)

seen that in general, the model predicts for most soils a too weak pH dependent B solubility when compared to the experimental data. This is most pronounced for the soils with the lowest organic matter content, namely soil D1 and D4. With increasing pH, the model calculates on average a decrease in B concentration of 0.65 µmol L^{-1} pH^{-1} when all 10 soils are considered, which is lower than the 1.84 µmol L^{-1} pH^{-1} found based on the experimental data. Based on the pH dependent B speciation, it seems that B adsorption to organic matter at high pH is underestimated by the model.

4. Conclusions

In this study, we used a multi-surface model to understand the chemical speciation of B in soils, which includes B in solution as boric

acid and borate, and B bound to dissolved humic acids, as well as B adsorption on clay mineral edges, oxides and solid humic acids. Taking the B measured in 0.01 M $CaCl_2$ as the starting point, reactive B was calculated with the model as the sum of dissolved and adsorbed B. Our results show that these calculations are most comparable to the reactive B concentration estimated by a 0.05 M KH_2PO_4 extraction for the soils in this study. The alternative 0.43 M HNO_3 and 0.2 mannitol +0.1 M TEA buffer extractions resulted in higher estimates of reactive B concentrations, probably due to dissolution of B-containing Si, Fe and Al minerals and/or due to the formation of colloidal particles because of the low salt level in the latter extraction solution. Caution should thus be taken when using these extraction methods to quantify reactive B for determination of plant available B. For the mannitol extraction, changes in the extraction protocol (e.g. concentration, change of buffer solution, addition of salts) might lead to better measurements of reactive B that is potentially available for plant uptake.

Measurements of pH dependent B solubility showed that the B in 0.01 M $CaCl_2$ decreases with increasing pH. Except for two soil samples, the largest decrease in B concentration with increasing pH was found for the soils with the highest organic carbon content. This is also predicted by the model, due to an increase in B adsorption with an increase in pH. The multi-surface model tends to underestimate the adsorption of B by organic matter at higher pH values, resulting in a weaker pH dependency predicted by the model than shown by the experimental data.

Speciation calculations based on our model show that oxides are most important for B adsorption in acidic soil from the humid tropics, while organic matter is more important for temperate and high pH soils. However, the interaction of the natural reactive B with the solid phase is limited for soils with pH($CaCl_2$) lower than 6. Future studies should focus on non-equilibrium processes that buffer bioavailable B in agricultural top soils, such as organic matter mineralization and mineral weathering. These results will further enhance the understanding of B speciation and bioavailability in soils, and improve the development of B management strategies.

Declaration of competing interest

The authors declare that they have no known competing financial interests or personal relationships that could have appeared to influence the work reported in this paper.

Acknowledgements

This work was supported by NWO (grant number 14688, 'Micronutrients for better yields'). The Dutch soil samples were sampled and provided by Nutrient Management Institute, The Netherlands in the framework of the NWO project 'Micronutrient Management for Sustainable Agriculture and Environment' (grant number 10707). Soil samples from Burundi were collected by IFDC (the International Fertilizer Development Centre) in the framework of the PAPAB project, and sent to Wageningen for analyses. All analyses were done in the CBLB laboratory in Wageningen University and Research, except for the total element concentrations which were measured at ECN-TNO in Petten. We greatly appreciate the help and expertise of Peter Nobels for the ICP measurements of boron in the different extraction solutions.

Appendix A. Supplementary data

Supplementary data to this article can be found online at https://doi.org/10.1016/j.apgeochem.2020.104797.

References

Aitken, R.L., Jeflrey, A.J., Compton, B.L., 1987. Evaluation of selected extractants for boron in some queensland soils. Aust. J. Soil Res. 25 (3), 263–273.

Bassett, R.L.L., 1980. A critical evaluation of the thermodynamic data for boron ions, ion pairs, complexes, and polyanions in aqueous solution at 298.15 K and 1 bar. Geochem. Cosmochim. Acta 44, 1151–1160. https://doi.org/10.1016/0016-7037(80)90069-1.

Bibi, I., Singh, B., Silvester, E., 2012. Mineralogy and Acid Neutralisation Mechanisms in Inland Acid Sulfate Environments. University of Sydney.

Bibi, I., Singh, B., Silvester, E., 2011. Dissolution of illite in saline–acidic solutions at 25 °C. Geochem. Cosmochim. Acta 75, 3237–3249. https://doi.org/10.1016/J.GCA.2011.03.022.

Bingham, F.T., 1982. Boron. In: Page, A.L., Miller, M.H., Keeny, D.R. (Eds.), Methods of Soil Analysis Part 2 Chemical and Mineralogical Properties. American Society of Agronomy, Madison, pp. 431–448.

Bourne, E.J., Hutson, D.H., Weigel, H., 1961. 7. Complexes between molybdate and acyclic polyhydroxy-compounds. J. Chem. Soc. 35. https://doi.org/10.1039/jr9610000035, 0.

Chao, T.T., Sanzolone, R.F., 1989. Fractionation of soil selenium by sequential partial dissolution. Soil Sci. Soc. Am. J. 53, 385. https://doi.org/10.2136/sssaj1989.03615995005300020012x.

Chaudhary, D.R., Shukla, L., 2003. Availability of soil boron fractions to mustard [Brassica juncea (L.) Czern.] in arid soils of Rajasthan (India). Agrochimica 173–179.

Cividini, D., Lemarchand, D., Chabaux, F., Boutin, R., Pierret, M.-C., 2010. From biological to lithological control of the B geochemical cycle in a forest watershed (Strengbach, Vosges). Geochem. Cosmochim. Acta 74, 3143–3163. https://doi.org/10.1016/j.gca.2010.03.002.

Couch, E.L., 1971. Calculation of paleosalinities from boron and clay mineral data. Am. Assoc. Petrol. Geol. Bull. 55.

Cui, Y., Weng, L., 2013. Arsenate and phosphate adsorption in relation to oxides composition in soils: LCD modeling. Environ. Sci. Technol. 47, 7269–7276. https://doi.org/10.1021/es400526q.

Degryse, F., Broos, K., Smolders, E., Merckx, R., 2003. Soil solution concentration of Cd and Zn can be predicted with a CaCl 2 soil extract. Eur. J. Soil Sci. 54, 149–158. https://doi.org/10.1046/j.1365-2389.2003.00503.x.

Degryse, F., Smolders, E., Parker, D.R., 2009. Partitioning of metals (Cd, Co, Cu, Ni, Pb, Zn) in soils: concepts, methodologies, prediction and applications - a review. Eur. J. Soil Sci. 60, 590–612. https://doi.org/10.1111/j.1365-2389.2009.01142.x.

Dijkstra, J.J., Meeussen, J.C.L., Comans, R.N.J., 2009. Evaluation of a generic multisurface sorption model for inorganic soil contaminants. Environ. Sci. Technol. 43, 6196–6201. https://doi.org/10.1021/es900555g.

Doleźal, J., Klausen, K.S., Langymyhr, F.J., 1973. Studies in the complex formation of metal ions with sugars : Part I. The complex formation of cobalt(II), cobalt(III), copper(II) and nickel(II) with mannitol. Anal. Chim. Acta 63, 71–77. https://doi.org/10.1016/S0003-2670(01)82175-9.

Doleźal, J., Langmyhr, F.J., 1972. Some possibilities of redox titrations with iron(ii) sulphate in an alkaline mannitol medium. Anal. Chim. Acta 61, 73–81. https://doi.org/10.1016/S0003-2670(01)81927-9.

Dordas, C., Chrispeels, M.J., Brown, P.H., 2000. Permeability and channel-mediated transport of boric acid across membrane vesicles isolated from squash roots. Plant Physiol. 124, 1349–1361. https://doi.org/10.1104/pp.124.3.1349.

Fruchter, J.S., Ral, D., Zachara, J.M., 1990. Identification of solubility-controlling solid phases in a large fly ash field lysimeter. Environ. Sci. Technol. 24, 1173–1179. https://doi.org/10.1021/es00078a004.

Gaillardet, J., Lemarchand, D., 2018. Boron in the Weathering Environment. Springer, Cham, pp. 163–188. https://doi.org/10.1007/978-3-319-64666-4_7.

Goldberg, S., 2014a. Chemical modeling of boron adsorption by humic materials using the constant capacitance model. Soil Sci. 179, 561–567. https://doi.org/10.1097/SS.0000000000000098.

Goldberg, S., 2014b. Application of surface complexation models to anion adsorption by natural materials. Environ. Toxicol. Chem. 33, 2172–2180. https://doi.org/10.1002/etc.2566.

Goldberg, S., 2004. Modeling boron adsorption isotherms and envelopes using the constant capacitance model. Vadose Zone J. 3, 676–680. https://doi.org/10.2136/vzj2004.0676.

Goldberg, S., 1999. Reanalysis of boron adsorption on soils and soil minerals using the constant capacitance model. Soil Sci. Soc. Am. J. 63, 823–829. https://doi.org/10.2136/sssaj1999.634823x.

Goldberg, S., 1997. Reactions of boron with soils. Plant Soil 193, 35–48. https://doi.org/10.1023/A:1004203723343.

Goldberg, S., Corwin, D.L., Shouse, P.J., Suarez, D.L., 2005. Prediction of boron adsorption by field samples of diverse textures. Soil Sci. Soc. Am. J. 69, 1379–1388.

Goldberg, S., Forster, H.S., Heick, E.L., 1993. Boron adsorption mechanisms on oxides, clay minerals, and soils inferred from ionic strength effects. Soil Sci. Soc. Am. J. 57, 704. https://doi.org/10.2136/sssaj1993.03615995005700030013x.

Goldberg, S., Forster, H.S., Lesch, S.M., Heick, E.L., 1996. Influence of anion competition on Boron adsorption by clays and soils. Soil Sci. 161, 99–103. https://doi.org/10.1097/00010694-199602000-00003.

Goldberg, S., Glaubig, R., 1986a. Boron adsorption on California soils. Soil Sci. Soc. Am. 50, 1173–1176.

Goldberg, S., Glaubig, R.A., 1986b. Boron adsorption and silicon release by the clay minerals kaolinite, montmorillonite, and Illite1. Soil Sci. Soc. Am. J. 50, 1442. https://doi.org/10.2136/sssaj1986.03615995005000060013x.

Goldberg, S., Glaubig, R.A., 1985. Boron adsorption on aluminum and iron oxide minerals 1. Soil Sci. Soc. Am. J. 49, 1374–1379.

Goldberg, S., Lesch, S.M., Suarez, D.L., 2000. Predicting boron adsorption by soils using soil chemical parameters in the constant capacitance model. Soil Sci. Soc. Am. J. 64, 1356. https://doi.org/10.2136/sssaj2000.6441356x.

Goldberg, S., Suarez, D.L., 2014. A new soil test for quantitative measurement of available and adsorbed boron. Soil Sci. Soc. Am. J. 78, 480. https://doi.org/10.2136/sssaj2013.09.0404.

Goldberg, S., Suarez, D.L., Basta, N.T., Lesch, S.M., 2004. Predicting boron adsorption isotherms by midwestern soils using the constant capacitance model. Soil Sci. Soc. Am. J. 68, 137–142.

Goli, E., Hiemstra, T., Rahnemaie, R., 2019. Interaction of boron with humic acid and natural organic matter: experiments and modeling. Chem. Geol. 515, 1–8. https://doi.org/10.1016/J.CHEMGEO.2019.03.021.

Goli, E., Rahnemaie, R., Hiemstra, T., Malakouti, M.J., 2011. The interaction of boron with goethite: experiments and CD-MUSIC modeling. Chemosphere 82, 1475–1481. https://doi.org/10.1016/j.chemosphere.2010.11.034.

Groenenberg, J.E., Lofts, S., 2014. The use of assemblage models to describe trace element partitioning, speciation, and fate: a review. Environ. Toxicol. Chem. 33, 2181–2196. https://doi.org/10.1002/etc.2642.

Groenenberg, J.E., Römkens, P.F.A.M., Zomeren, A. Van, Rodrigues, S.M., Comans, R.N. J., 2017. Evaluation of the single dilute (0.43 M) nitric acid extraction to determine geochemically reactive elements in soil. Environ. Sci. Technol. 51, 2246–2253. https://doi.org/10.1021/acs.est.6b05151.

Gu, B., Lowe, L.E., 1990. Studies on the ad sorption of boron on humic acids. Can. J. Soil Sci. 70, 305–311. https://doi.org/10.4141/cjss90-031.

Gupta, U.C., Jame, Y.W., Campbell, C.A., Leyshon, A.J., Nicholaichuk, AnW., 1985. Boron toxicity and deficiency: a review. Can. J. Soil Sci. 65, 381–409.

Hass, A., Loeppert, R.H., Messina, M.G., Rogers, T.D., 2011. Determination of phosphate in selective extractions for soil iron oxides by the molybdenum blue method in an automated continuance flow injection system. Commun. Soil Sci. Plant Anal. 42, 1619–1635. https://doi.org/10.1080/00103624.2011.584598.

Heidmann, I., Christl, I., Leu, C., Kretzschmar, R., 2005. Competitive sorption of protons and metal cations onto kaolinite: experiments and modeling. J. Colloid Interface Sci. 282, 270–282. https://doi.org/10.1016/J.JCIS.2004.08.019.

Hengl, T., Mendes de Jesus, J., Heuvelink, G.B.M., Ruiperez Gonzalez, M., Kilibarda, M., Blagotić, A., Shangguan, W., Wright, M.N., Geng, X., Bauer-Marschallinger, B., Guevara, M.A., Vargas, R., MacMillan, R.A., Batjes, N.H., Leenaars, J.G.B., Ribeiro, E., Wheeler, I., Mantel, S., Kempen, B., 2017. SoilGrids250m: global gridded soil information based on machine learning. PloS One 12, e0169748. https://doi.org/10.1371/journal.pone.0169748.

Hiemstra, T., 2018. Ferrihydrite interaction with silicate and competing oxyanions: geometry and Hydrogen bonding of surface species. Geochem. Cosmochim. Acta 238, 453–476. https://doi.org/10.1016/J.GCA.2018.07.017.

Hiemstra, T., Antelo, J., Rahnemaie, R., van Riemsdijk, W.H., 2010. Nanoparticles in natural systems I: the effective reactive surface area of the natural oxide fraction in field samples. Geochem. Cosmochim. Acta 74, 41–58. https://doi.org/10.1016/j.gca.2009.10.018.

Hiemstra, T., Mia, S., Duhaut, P.B., Molleman, B., 2013. Natural and pyrogenic humic acids at goethite and natural oxide surfaces interacting with phosphate. Environ. Sci. Technol. 47, 9182–9189. https://doi.org/10.1021/es400997n.

Hiemstra, T., Van Riemsdijk, W.H., 2009. A surface structural model for ferrihydrite I: sites related to primary charge, molar mass, and mass density. Geochem. Cosmochim. Acta 73, 4423–4436. https://doi.org/10.1016/j.gca.2009.04.032.

Hiemstra, T., Zhao, W., 2016. Reactivity of ferrihydrite and ferritin in relation to surface structure, size, and nanoparticle formation studied for phosphate and arsenate. Environ. Sci. Nano 3, 1265–1279. https://doi.org/10.1039/C6EN00061D.

Hou, J., Evans, L.J., Spiers, G.A., 1995. Chemical fractionation of soil boron: l. Method development. Can. J. Soil Sci. 76, 485–491.

Hou, J., Evans, L.J., Spiers, G.A., 1994. Boron fractionation in soils. Commun. Soil Sci. Plant Anal. 25, 1841–1853. https://doi.org/10.1080/00103629409369157.

Houba, V.J.G., Temminghoff, E.J.M., Gaikhorst, G.A., van Vark, W., 2000. Soil analysis procedures using 0.01 M calcium chloride as extraction reagent. Commun. Soil Sci. Plant Anal. 31, 1299–1396. https://doi.org/10.1080/00103620009370514.

Howe, P.D., 1998. A review of boron effects in the environment. Biol. Trace Elem. Res. 66, 153–166.

Huertas, F.J., Chou, L., Wollast, R., 1999. Mechanism of kaolinite dissolution at room temperature and pressure Part II: kinetic study. Geochem. Cosmochim. Acta 63, 3261–3275. https://doi.org/10.1016/S0016-7037(99)00249-5.

ISO, 2016. Soil Quality 17586:2016 – Extraction of Trace Elements Using Dilute Nitric Acid.

ISO, 2012. ISO 12782-3:2012 Soil Quality – Parameters for Geochemical Modelling of Leaching and Speciation of Constituents in Soils and Materials – Part 3: Extraction of Aluminium Oxides and Hydroxides with Ammonium Oxalate/oxalic Acid.

Jin, J., Martens, D.C., Zelazny, L.W., 1987. Distribution and plant availability of soil boron fractions. Soil Sci. Soc. Am. J. 51, 1228. https://doi.org/10.2136/sssaj1987.03615995005100050025x.

Jørgensen, C., Turner, B.L., Reitzel, K., 2015. Identification of inositol hexakisphosphate binding sites in soils by selective extraction and solution 31P NMR spectroscopy. Geoderma 257–258, 22–28. https://doi.org/10.1016/j.geoderma.2015.03.021.

Kabata-Pendias, A., Pendias, H., 2001. Trace Elements in Soils and Plants, third ed.

Kaplan, D.I., Sumner, M.E., Bertsch, P.M., Adriano, D.C., 1996. Chemical conditions conducive to the release of mobile colloids from ultisol profiles. Soil Sci. Soc. Am. J. 60, 269–274. https://doi.org/10.2136/sssaj1996.03615995006000010041x.

Karlsson, P.M., Postmus, B.R., Palmqvist, A.E.C., 2009. Dissolution and protection of aluminium oxide in corrosive aqueous media-an ellipsometry and reflectometry study. J. Dispersion Sci. Technol. 30, 949–953. https://doi.org/10.1080/01932690802646363.

Keizer, M.G., Van Riemsdijk, W.H., 1995. ECOSAT, a Computer Program for the Calculation of Chemical Speciation and Transport in Soil-Water Systems (Wageningen, the Netherlands).

Keren, R., Bingham, F.T., Rhoades, J.D., 1985. Plant uptake of boron as affected by boron distribution between liquid and solid phases in soil. Soil Sci. Soc. Am. J. 49, 297–302. https://doi.org/10.2136/sssaj1985.03615995004900020004x.

Keren, R., Communar, G., 2009. Boron sorption on wastewater dissolved organic matter: pH effect. Soil Sci. Soc. Am. J. 73, 2021–2025. https://doi.org/10.2136/sssaj2008.0381.

Keren, R., Mezuman, U., 1981. Boron adsorption by clay minerals using a phenomenological equation. Clay Clay Miner. 29, 198–204. https://doi.org/10.1346/CCMN.1981.0290305.

Kinniburgh, D.G.D.G., Milne, C.J.C.J., Benedetti, M.F., Pinheiro, J.P., Filius, J., Koopal, L. K.L.K., Van Riemsdijk, Willem, H., Riemsdijk, W.H., 1996. Metal ion binding by humic acid: application of the NICA-donnan model. Environ. Sci. Technol. 30, 1687–1698. https://doi.org/10.1021/es950695h.

Kinrade, S.D., Del Nin, J.W., Schach, A.S., Sloan, T.A., Wilson, K.L., G Knight, C.T., 1999. Stable five-and six-coordinated silicate anions in aqueous solution. Science 285, 1542–1545.

Knoeck, J., Taylor, J.K., 1969. Aqueous boric acid-borate-mannitol equilibria. Anal. Chem. 41, 1730–1734. https://doi.org/10.1021/ac60282a005.

Köhler, S.J., Dufaud, F., Oelkers, E.H., 2003. An experimental study of illite dissolution kinetics as a function of ph from 1.4 to 12.4 and temperature from 5 to 50°C. Geochem. Cosmochim. Acta 67, 3583–3594. https://doi.org/10.1016/S0016-7037(03)00163-7.

Konert, M., Vandenberghe, J., 1997. Comparison of laser grain size analysis with pipette and sieve analysis: a solution for the underestimation of the clay fraction. Sedimentology 44, 523–535.

Kot, F.S., Farran, R., Fujiwara, K., Kharitonova, G.V., Kochva, M., Shaviv, A., Sugo, T., 2016. On boron turnover in plant–litter–soil system. Geoderma 268, 139–146. https://doi.org/10.1016/J.GEODERMA.2016.01.022.

Kot, F.S., Farran, R., Kochva, M., Shaviv, A., 2012. Boron in humus and inorganic components of Hamra and Grumosol soils irrigated with reclaimed wastewater. Soil Res. 50, 30–43. https://doi.org/10.1071/SR11232.

Kretzschmar, R., Sticher, H., 1998. Colloid transport in natural porous media: influence of surface chemistry and flow velocity. Phys. Chem. Earth 23, 133–139. https://doi.org/10.1016/S0079-1946(98)00003-2.

Kutus, B., Ozsvár, D., Varga, N., Pálinkó, I., Sipos, P., 2017. ML and ML $_2$ complex formation between Ca(ii) and d -glucose derivatives in aqueous solutions. Dalton Trans. 46, 1065–1074. https://doi.org/10.1039/C6DT04356A.

Lemarchand, D., Cividini, D., Turpault, M.-P., Chabaux, F., 2012. Boron isotopes in different grain size fractions: exploring past and present water–rock interactions from two soil profiles (Strengbach, Vosges Mountains). Geochem. Cosmochim. Acta 98, 78–93. https://doi.org/10.1016/J.GCA.2012.09.009.

Lemarchand, E., Schott, J., Gaillardet, J., 2005. Boron isotopic fractionation related to boron sorption on humic acid and the structure of surface complexes formed. Geochem. Cosmochim. Acta 69, 3519–3533.

Lindsay, W.L., 1979. Chemical Equilibria in Soils. Wiley, New York.

Lindsay, W.L., Norvell, W.A., 1978. Development of a DTPA soil test for zinc, iron, manganese, and Copper1. Soil Sci. Soc. Am. J. 42, 421. https://doi.org/10.2136/sssaj1978.03615995004200030009x.

Manning, B.A., Goldberg, S., 1996. Modeling competitive adsorption of arsenate with phosphate and molybdate on oxide minerals. Repr. from Soil Sci. Soc. Am. J. Vol. GO South Segoe Rd 60, 121–131.

Marzadori, C., Antisari, L.V., Ciavatta, C., Sequi, P., 1991. Soil organic matter influence on adsorption and desorption of boron. Soil Sci. Soc. Am. J. 55, 1582. https://doi.org/10.2136/sssaj1991.03615995005500060013x.

Mendez, J.C., Hiemstra, T., 2020a. Ternary complex formation of phosphate with Ca and Mg ions binding to ferrihydrite: experiments and mechanisms. ACS Earth Sp. Chem. 4 (4), 545–557. https://doi.org/10.1021/acsearthspacechem.9b00320.

Mendez, J.C., Hiemstra, T., 2020b. High and low affinity sites of ferrihydrite for metal ion adsorption: data and modeling of the alkaline-earth ions Be, Mg, Ca, Sr, Ba, and Ra. Geochem. Cosmochim. Acta. https://doi.org/10.1016/j.gca.2020.07.032.

Mendez, J.C., Hiemstra, T., 2018. Carbonate adsorption to ferrihydrite: competitive interaction with phosphate for use in soil systems. ACS Earth Sp. Chem. 3 (1), 129–141. https://doi.org/10.1021/acsearthspacechem.8b00160.

Mendez, J.C., Hiemstra, T., Koopmans, G.F., 2020. Assessing the reactive surface area of soils and the association of soil organic carbon with natural oxide nanoparticles using ferrihydrite as proxy. Environ. Sci. Technol. 9, 2020. https://doi.org/10.1021/acs.est.0c02163.

Mertens, J., Van Laer, L., Salaets, P., Smolders, E., 2011. Phytotoxic doses of boron in contrasting soils depend on soil water content. Plant Soil 342, 73–82. https://doi.org/10.1007/s11104-010-0666-x.

Milne, C.J., Kinniburgh, D.G., van Riemsdijk, W.H., Tipping, E., 2003. Generic NICA–Donnan model parameters for metal-ion binding by humic substances. Environ. Sci. Technol. 37, 958–971. https://doi.org/10.1021/es0258879.

Mohr, S., Bechtold, T., 2001. Electrochemical behaviour of iron-complexes in presence of competitive ligands: a strategy for optimization of current density. J. Appl. Electrochem. 31, 363–368.

Murphy, J., Riley, J.P., 1962. A modified single solution method for the determination of phosphate in natural waters. Anal. Chim. Acta 27, 31–36. https://doi.org/10.1016/S0003-2670(00)88444-5.

NEN 5753, 2018. Soil - Determination of Clay Content and Particle Distribution in Soil and Sediment by Sieve and Pipet, 2018.

Noireaux, J., Gaillardet, J., Sullivan, P.L., Brantley, S.L., 2014. Boron isotope fractionation in soils at shale hills CZO. Procedia Earth Planet. Sci. 10, 218–222. https://doi.org/10.1016/J.PROEPS.2014.08.024.

Novozamsky, I., Barrera, L.L., Houba, V.J.G., van der Lee, J.J., van Eck, R., 1990. Comparison of a hot water and cold 0.01 M Cacl $_2$ extraction procedures for the determination of boron in soil. Commun. Soil Sci. Plant Anal. 21, 2189–2195. https://doi.org/10.1080/00103629009368370.

Park, H., Schlesinger, W.H., 2002. Global biogeochemical cycle of boron. Global Biogeochem. Cycles 16. https://doi.org/10.1029/2001GB001766, 20-21-20–11.

Parks, J.L., Edwards, M., 2005. Boron in the environment. Crit. Rev. Environ. Sci. Technol. 35, 81–114. https://doi.org/10.1080/10643380590900200.

Peak, D., Luther, G.W., Sparks, D.L., 2003. ATR-FTIR spectroscopic studies of boric acid adsorption on hydrous ferric oxide. Geochem. Cosmochim. Acta 67, 2551–2560. https://doi.org/10.1016/S0016-7037(03)00096-6.

Pédrot, M., Dia, A., Davranche, M., Bouhnik-Le Coz, M., Henin, O., Gruau, G., 2008. Insights into colloid-mediated trace element release at the soil/water interface. J. Colloid Interface Sci. 325, 187–197. https://doi.org/10.1016/j.jcis.2008.05.019.

Pokrovsky, O., Schott, J., 2002. Iron colloids/organic matter associated transport of major and trace elements in small boreal rivers and their estuaries (NW Russia). Chem. Geol. 190, 141–179. https://doi.org/10.1016/S0009-2541(02)00115-8.

Sarkar, D., De, D.K., Das, R., Mandal, B., 2014. Removal of organic matter and oxides of iron and manganese from soil influences boron adsorption in soil. Geoderma 214–215, 213–216. https://doi.org/10.1016/j.geoderma.2013.09.009.

Scopes, R.K., 1994. Protein Purification: Principles and Practice, third ed. Springer Science & Business Media.

Shorrocks, V.M., 1997. The occurrence and correction of boron deficiency. Plant Soil 193, 121–148. https://doi.org/10.1023/A:1004216126069.

Sims, J.R., Bingham, F.T., 1967. Retention of boron by layer silicates, sesquioxides, and soil materials: I. Layer Silicates1. Soil Sci. Soc. Am. J. 31, 728. https://doi.org/10.2136/sssaj1967.03615995003100060010x.

Sparks, D.L., 1996. Soil science society of America. In: Methods of Soil Analysis. Part 3, Chemical Methods. Soil Science Society of America. L.E., American Society of Agronomy., D.L., Page, A.L., Helmke, P.A., Loeppert, R.H., Soltanpour, P.N., Tabatabai, M.A., Johnston, C.T., Sumner, M.E.

Su, C., Suarez, D.L., 2004. Boron release from weathering of illites, serpentine, shales, and illitic/palygorskitic soils. Soil Sci. Soc. Am. J. 68, 96–105.

Su, C., Suarez, D.L., 1995. Coordination of adsorbed boron: a ftir spectroscopic study. Environ. Sci. Technol. 29, 302–311. https://doi.org/10.1021/es00002a005.

Uluisik, I., Karakaya, H.C., Koc, A., 2018. The importance of boron in biological systems. J. Trace Elem. Med. Biol. 45, 156–162. https://doi.org/10.1016/J.JTEMB.2017.10.008.

Van Eynde, E., Mendez, J.C., Hiemstra, T., Comans, R.N.J., 2020. Boron adsorption to ferrihydrite with implications for surface speciation in soils: experiments and modeling. ACS Earth Sp. Chem. acsearthspacechem. https://doi.org/10.1021/acsearthspacechem.0c00078, 0c00078.

van Zomeren, A., Comans, R.N.J., 2007. Measurement of humic and fulvic acid concentrations and dissolution properties by a rapid batch procedure. Environ. Sci. Technol. 41, 6755–6761. https://doi.org/10.1021/es0709223.

Vaughan, B., Howe, & J., 1994. Evaluation of boron chelates in extracting soil boron. Commun. Soil Sci. Plant Anal. 25, 1071–1084. https://doi.org/10.1080/00103629409369099.

Weng, L., Temminghoff, E.J.M., Van Riemsdijk, W.H., 2001. Contribution of individual sorbents to the control of heavy metal activity in sandy soil. Environ. Sci. Technol. 35, 4436–4443. https://doi.org/10.1021/es010085j.

Wolf, A.M., Baker, D.E., 1990. Colorimetric method for phosphorus measurement in ammonium oxalate soil extracts. Commun. Soil Sci. Plant Anal. 21, 2257–2263. https://doi.org/10.1080/00103629009368378.

Xu, D., Peak, D., 2007. Adsorption of boric acid on pure and humic acid coated am-Al(OH)3: a boron K-edge XANES study. Environ. Sci. Technol. 41, 903–908. https://doi.org/10.1021/ES0620383.